NAVAL POSTGRADUATE SCHOOL
Monterey, California

THESIS

AN EXPERIMENTAL TESTBED FOR A FREE-FLOATING MANIPULATOR

by

Douglas Lamar Maddox

December 1993

Thesis Advisor: Ranjan Mukherjee

REPORT DOCUMENTATION PAGE

Form Approved OMB No. 0704

1. AGENCY USE ONLY	2. REPORT DATE 16 December 1993	3. REPORT TYPE AND DATES COVERED Master's Thesis

4. TITLE AND SUBTITLE: AN EXPERIMENTAL TESTBED FOR A FREE-FLOATING MANIPULATOR

5. FUNDING NUMBERS

6. AUTHOR(S) *Maddox, Douglas Lamar*

7. PERFORMING ORGANIZATION NAME(S) AND ADDRESS(ES)
Naval Postgraduate School
Monterey, CA 93943-5000

8. PERFORMING ORGANIZATION REPORT NUMBER

9. SPONSORING/MONITORING AGENCY NAME(S) AND ADDRESS(ES)

10. SPONSORING/MONITORING AGENCY REPORT NUMBER

11. SUPPLEMENTARY NOTES The views expressed in this thesis are those of the author and do not reflect the official policy or position of the Department of Defense or the U.S. Government.

12a. DISTRIBUTION/AVAILABILITY STATEMENT
Approved for public release; distribution is unlimited.

12b. DISTRIBUTION CODE
*A

13.
ABSTRACT

The attitude control of a multibody system in a gravity free environment has been an ongoing field of study for decades. Although most methods involve the use of thrusters, some algorithms exist that utilize internal motion of the system for reorientation. These algorithms reduce the expenditure of the limited amount of on board fuel so as to extend the useful life span of the system. An experimental facility for testing existing algorithms, and algorithms to be developed in the future for motion planning of multibody space systems, is developed as part of this research. The multibody system developed is comprised of a two link space vehicle/manipulator system. The system is mounted on air bearings and floats freely on a flat glass table. The robotic system is controlled in real time using a VME based controller with support from a SPARC station.

14. SUBJECT TERMS
Free-Floating, Space Robot Manipulator, Real-Time Control, Experimental Testbed

15. NUMBER OF PAGES 44

16. PRICE CODE

17. SECURITY CLASSIFICATION OF REPORT	18. SECURITY CLASSIFICATION OF THIS PAGE	19. SECURITY CLASSIFICATION OF ABSTRACT	20. LIMITATION OF ABSTRACT
Unclassified	Unclassified	Unclassified	UL

NSN 7540-01-280-5500

Standard Form 298 (Rev. 2-89)
Prescribed by ANSI STD. 239-18

Approved for public release; distribution is unlimited.

An Experimental Testbed for a Free-Floating Manipulator

by

Douglas L. Maddox
Lieutenant, United States Navy
B.S., Georgia Institute of Technology, 1984

Submitted in partial fulfillment
of the requirements for the degree of

MASTER OF SCIENCE IN MECHANICAL ENGINEERING

from the

NAVAL POSTGRADUATE SCHOOL
December 1993

Author: 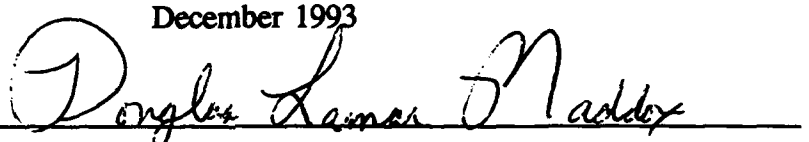
Douglas Lamar Maddox

Approved by: 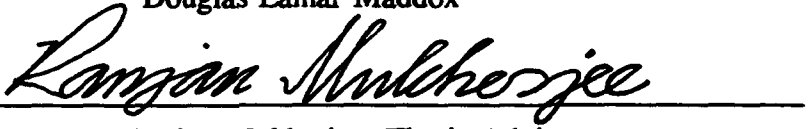
Ranjan Mukherjee, Thesis Advisor

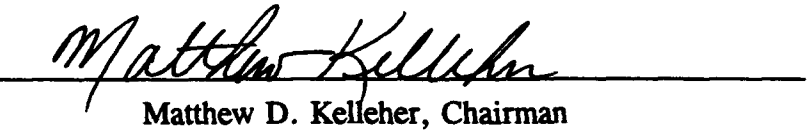
Matthew D. Kelleher, Chairman
Department of Mechanical Engineering

ABSTRACT

The-attitude control of a multibody system in a gravity free environment has been an ongoing field of study for decades. Although most methods involve the use of thrusters, some algorithms exist that utilize internal motion of the system for reorientation. These algorithms reduce the expenditure of the limited amount of onboard fuel so as to extend the useful life span of the system. An experimental facility for testing existing algorithms, and algorithms to be developed in the future for motion planning of multibody space systems, is developed as part of this research. The multibody system developed is comprised of a two link space vehicle/manipulator system. The system is mounted on air bearings and floats freely on a flat glass table. The robotic system is controlled in real time using a VME based controller with support from a SPARC station.

TABLE OF CONTENTS

ACKNOWLEDGMENTS

This thesis is dedicated to my daughters, Meghan and Kaylin, the loves of my life and to Martine Gish who bathed, fed, clothed, and spent countless hours with Meghan and Kaylin and who read through version after version of this work and patiently listened to my presentation over and over again. I love you.

A special thanks to LCDR Craig Bateman, whose ability to see the forest for the trees often provided the bridge between theoretical and practical engineering and to the engineers and technicians in the Engineering and Machine shop of the Naval Postgraduate School's Department of Mechanical Engineering for the countless hours and dollars saved and for their superb workmanship.

I would also like to acknowledge Mr. Guy Bigwood of AMEROPEAN Corp., and Mr. Fred Moritz of MFM Technology, INC., and thank them for their technical guidance and expedient service.

Last, but certainly not least, I would like to express my gratitude to, and admiration for, Professor Ranjan Mukherjee whose uncanny ability to know just when to tether the umbilical chord provided me with a wide open learning environment. I truly had fun working on this thesis.

I. INTRODUCTION

The control of position and orientation of a multibody system in a gravity free environment has been an ongoing field of study for decades. Numerous algorithms exist which can adequately position a body given that there is one actuator for every articulated joint. These actuators work in conjunction with the many thrusters available for global positioning and fast orientation maneuvers. Algorithms have been developed to reorient a multibody system in space without the use of thrusters. These include controlling a satellite with two or more rotors [Ref 1: pp 21-25] and reconfiguration of a manipulator using internal motion [Ref.2, Ref. 3, Ref. 4]. The purpose of these algorithms is to reduce the expenditure of the limited amount of onboard fuel so as to extend the useful life span of the system. The focus of this thesis is to provide the researcher with an experimental testbed that can be used to test existing algorithms and future algorithms that will be developed, that reduce the need for thrusters in free floating manipulators.

The goal of this first chapter is to provide an understanding of the steps involved in the development of the testbed. Discussed in detail are the mechanical design of the robotic system from the dynamical equations, the choice of actuators and drives to meet the task requirements, and the controller cards along with associated software and additional hardware for real time computer control of the system. Chapter II is devoted to the mechanical design of the manipulator. The details of the components are explored as are the kinematic and dynamic parameters of the linkages chosen. The dynamical equations are used to obtain an upper bound for the torque requirement of the actuators for a large range of feasible motion. The harmonic drives of the actuators are then chosen appropriately to select compact motors that can meet the torque and speed requirements. Chapter III lists all the associated mechanical components such as the air pads, the table which supports the manipulator, the air system and the assembly of the components. Chapter IV is dedicated to the computer hardware and software requirements, and goes into some detail concerning capabilities that will be important for future experiments.

The heart of the control system is the Robot Control System (RCS). The RCS allows a source program, written in C to be compiled on the SPARCstation and downloaded to the memory of a real time computer, part of the Robot Controller Card (RCC). The CPU of the RCC runs the executable code and updates its commands to the robot in a closed loop control scheme. A program written in C on the SPARCstation, that was downloaded on the RCC for position control of the robot's linkages using feedback from the encoders, verified the computer control link. Chapter V summarizes the achievements and also provides recommendations for future modifications of the testbed.

A. THE MECHANICAL DESIGN OF THE MANIPULATOR

The design of the testbed was motivated by the need for the experimental validation of the motion planning algorithm presented in [Ref. 2]. Since designing a testbed solely for one experiment is a financially unsound practice, serious consideration was given to expandability and adaptability for future experiments. In [Ref. 2] the motion planning algorithm was applied to a two degree of freedom planar space robot system. To verify the efficiency of the algorithm, a planar two link manipulator was designed. The goal of this thesis was to design a facility after the above mentioned model, and to measure the design's success by tracking some desired trajectory. Given that the testbed was to simulate a gravity free environment, consideration was first given to simplicity in order to minimize the effect of external forces on the system. The crucial task was the design and construction of the simplest testbed that would meet the requirements of [Ref. 2], ensure that all external forces were minimized, and maintain planar motion. To keep this in the simplest terms, a body with a two link appendage was examined. Figure 1(a) and Fig. 1(b) depict the general shape of the appended manipulator. The free body diagram in Fig. 2 was used to develop the closed form dynamical equations of the manipulator using Lagrange's equations.

In the mechanical design of the manipulator several assumptions were made for simplification and are discussed in detail in Chapter II. Aluminum was selected as the material for the body and its links due to weight and cost considerations. The dimensions

of the manipulator body and links were selected based on weight and aesthetic considerations. The maximum values of angular velocity and angular acceleration were chosen to determine an upper bound for the acctuator torques for a broad range of feasible motion. The maximum values of the actuator torques were provided to an outside engineering firm which selected and manufactured the required motor, harmonic drive reduction gear, encoder, and amplifier assembly. DC Brushless motors were used due to their inherent properties of high horsepower per volume of motor, longer life at high speed operations, low friction, and linear torque/speed relationship over wide ranges. Brushless motors were found to be particularly attractive because the elimination of brushes decreases the noise level that may interfere with electronic components [Ref 5]. Harmonic drive gear boxes were selected due to their compactness and very low backlash that degrades positioning accuracy. Even a small amount of backlash at a joint can lead to large errors at the manipulator tips [Ref. 5]. Optical encoders were installed to provide the necessary digital feedback of the mechanical motor position. This feedback is a crucial component in updating future commands to the motor for accurate manipulator positioning and trajectory tracking. Signals generated by the computer system to drive the motors are weak in strength. Therefore, amplifiers were provided to increase the input signal to the level required by the motors. These amplifiers require their own 48 volt, 12 ampere DC power supply which was purchased separately as a stock item. The final assemblies, shipped as two units, were the two DC brushless motor/harmonic drive reduction gear/optical encoder assemblies and their respective stand alone amplifiers.

The final mechanical components of the planar space robot to be discussed are the two needle thrust bearings. As mentioned previously, the testbed was developed for a perfectly planar motion. The body and links of the manipulator must move in a plane parallel to one another. To ensure parallel motion, needle thrust bearings were added between the manipulator's main body and link 1 and between link 1 and link 2. The bearings were positioned as shown in Fig. 1(b) and Fig. 3. More details concerning the purpose and installation of the bearings will be provided in Chapter II.

B. SIMULATING A GRAVITY FREE ENVIRONMENT IN 2-D

In order to simulate a gravity free environment the manipulator was required to float on a cushion of air. Numerous air pad designs are available from industrial sources. The selection of a suitable pad was primarily a function of the weight which the pads must support. The design of the manipulator determined the number and position of the air pads. Figure 1(a) and Fig. 1(b) depict the locations where the air pads were placed. Balance of the manipulator was best accomplished with three air pads. The weight of the manipulator is distributed roughly between the three pads. With a factor of safety incorporated, the size (surface area) of the air pads was determined based on the weight of the manipulator. A diagram, including the dimensions and weight of the manipulator and location of the air pads, was provided to an outside engineering firm which specializes in air bearings. The company provided the required air bearings. In general each pad is a 32mm, stainless steel disk that has a porous bronze ring through which air flows. Air is supplied at 5 atmospheres (72 psi) and leaves the bearings through the porous rings at a low volume but high velocity. The bearings are state of the art for their low air consumption, vibration free, and even air pattern displacement design [Ref. 6]. Chapter III will discuss the details of the air pads.

The air bearings require a flat, defect free surface. Granite tables exist which would satisfy this requirement but are expensive and extremely heavy. Glass was selected as a suitable substitute with the belief that its relatively smooth finish could provide an adequate operating surface. An aluminum structure, shown in Fig. 4, was designed to support a six foot square, one-half inch thick sheet of mirrored glass purchased from stock at a local glass distributor. The calculated weight of the manipulator and its accessories determined the glass thickness which in turn limited the glass quality [Ref. 7]. Adjustable leveling feet were added to the bottom of the support structure's legs and at two foot increments along the plane of the glass (see Fig. 4) to control the horizontal level of the glass. The glass was initially leveled in a gross manner by using a carpenter's bubble level and adjusting the leveling feet at the bottom of the support structure's legs. The glass level was then fine tuned by placing the free-floating manipulator at various

points on the glass surface then adjusting the two foot incremented leveling feet to eliminate any drift in the manipulator's transverse motion.

C. COMPUTER CONTROL OF THE MANIPULATOR

The next step was to select the necessary hardware and software that would, given an algorithm, generate the appropriate signals to the motor amplifiers using encoder feedback information. The position control of the manipulator must be performed in real time. For this purpose, the motion planning algorithm for the robot is programmed and compiled on a SPARCstation and downloaded in executable form to a real time controller card. The SPARCstation was selected because of its versatility, computing power, and due to existing compatible hardware and software in robotics controls. Details of the hardware and software are found in Chapter IV.

The SPARCstation has numerous features. It has all of the standard input/output ports, RAM, a compiler, and a UNIX operating system that is not a real time operating system. Attempting to control any trajectory of the manipulator for an extended period of time would be futile since the operating system of the SPARCstation would attempt to conduct its self checks and system updates and lose track of the current position and commands to the manipulators. The manipulators must be controlled in real time. A computer was chosen that has a relatively simple CPU that could receive, in its own assembly language, a compiled program from the SPARCstation and generate the required commands to drive the manipulator's motors. A VME card cage and a SBUS to VME adapter were purchased from a separate manufacturer. The adapter allows the compiled program from the SPARCstation to be passed to the CPU controller card. The card cage is the power source and housing for the various cards. Accompanying the CPU controller card are a digital to analog (and analog to digital) converter card as well as a separate card, termed as the position/velocity card, that receives the digital signal from the optical encoders. These two cards were placed in the card cage as well. A block diagram of the system is depicted in Fig. 5.

At the higher level, a programmer develops a program in C on the SPARCstation to implement a particular motion planning algorithm. The program is compiled and passed through the SBUS to VME adapter to the RCC (Robot Controller Card). The program is executed in the CPU that generates the necessary commands to drive the manipulator's motors. The signals are converted from digital to analog on a separate card. The signal is then amplified before being passed to the motors. The encoders provide feedback from the motors to the encoder receiver card. The signals are converted on the card and passed to the RCC where an error signal is generated. The error signal is subsequently used to generate the next set of commands to the motors. Specifics of the components described above are provided in Chapter IV.

D. A SUMMARY OF THE COMPONENTS

Although numerous miscellaneous items were used to tie each of the components together the major components are listed.

- SPARCstation LX with modified kernel for communication with the VME Card Cage and the Robot Controller Card (RCC)
- SBUS to VME Adapter
- VME card cage and power supply
- Robot Controller Card
- Digital to Analog (and analog to digital) Converter Card
- Position/Velocity Card for Optical Encoder feedback
- power supply for the motor amplifiers
- two amplifier/motor/reduction gear/encoder assemblies
- an aluminum space vehicle along with a two link manipulator
- two needle bearings
- three air bearings
- an air supply system, that delivers air at 72 psi, comprised of a 40 micron filter, a water separator, a desiccant air dryer, a regulator, and a five micron filter
- a glass table with an aluminum support structure

A detailed description of the accessory equipment used to connect each of the major components will be elaborated upon in the ensuing chapters. Almost all of these items were stock from local sources or manufactured at the Naval Postgraduate School Mechanical Engineering machine shop.

II. MECHANICAL DESIGN OF THE ROBOT

A. THE PLANAR SPACE ROBOT

In this part of Chapter II, the general shape of the planar space robot will be described. The shape of the robot is modeled after the free flying two dimensional space robot described in [Ref. 2]. The space robot was used as an example of a nonholonomic system whose motion could be planned by the "surface integral algorithm" developed in [Ref. 2].

1. General Shape of the Space Vehicle and Manipulator Links

Figure 2 is the same as that illustrated in [Ref. 2]. Figures 1(a) and 1(b) were derived from Fig. 2 and provide the actual shape of the space vehicle and manipulator links. Although weight, operating space limitations, and costs were instrumental in determining the robot's dimensions, aesthetics were also a primary consideration. In order to ensure planar motion of the space vehicle and manipulator links, link 1 was positioned on top of the space vehicle and link 2 as shown in Fig. 1(b). This positioning allowed the two actuating motors to be connected in the same manner at each joint which simplified the design considerably from other alternatives. Another advantage of this positioning is that it allowed for maximum angular displacement of the components relative to one another.

We decided to use a glass table six foot square in size to support the robotic system. The size of the table determined the size of the robot and its workspace. After a series of iterations the following dimensions (in centimeters) were chosen for the space vehicle/manipulator system.

TABLE 1. KINEMATIC PARAMETERS OF THE SPACE ROBOT

	Length/Radius	Width	Thickness
Space Vehicle	20	N/A	2.5
Link 1	40	6	2.5
Link 2	30	5	2.5

The manipulator links were tapered along their lengths and rounded at the ends for an anthropomorphic shape. The links were maneuvered by actuating motors placed at the link intersections. The mechanical design of the space robot required only link 1 to be machined to accommodate the body of the motor assemblies. An actuator was placed into the machined recesses at each end of link 1. Four mounting screws were then used to secure each motor to link 1. The output shaft of motor assembly #1 extends through link 1 and into the space vehicle where it is secured by a set screw. The output shaft of motor assembly #2 extends through link 1 and into link 2 where it is also secured by a set screw. The above method of mounting the actuators allowed for an unobstructed mounting surface for two needle roller bearings. The mounting of the bearings is shown in Fig. 3. The bearings will be discussed in later paragraphs.

2. Mathematical Model of the Space Robot for Determining the Actuator Torque Requirements and Harmonic Drive Reduction Ratios

In the initial considerations for the general shape of the space robot, the motor parameters were not necessary. Various manufacturer's catalogues were available to provide estimates of standard motor size and weights. But, the maximum torque which the actuators would be required to produce needed to be determined. Figure 2 illustrates the free body diagram used to model the planar space robot. The system can be described by five coordinates: x_0, y_0, θ_0 locating the center of mass and the orientation of the space vehicle, with θ_1 and θ_2 locating the angles of the manipulator links relative to the

axis of the space vehicle. The free body diagram in Fig. 2 was used to develop the closed form dynamical equations of the manipulator using Lagrange's equations. In order to simplify the calculations, link 1 was assumed to be fixed. The standard form of Lagrange's equation is [Ref. 8]:

$$\frac{\mathrm{d}}{\mathrm{dt}}\left(\frac{\partial \mathcal{L}}{\partial \dot{q}_i}\right) - \frac{\partial \mathcal{L}}{\partial q_i} = \tau_i \tag{1}$$

where q_i's are the generalized coordinates θ_1 and θ_2, $\mathcal{L} = \mathrm{T} - \mathrm{V}$ is defined as the Lagrangian, T=Total Kinetic Energy, V=Total Potential Energy, and τ_i's are the generalized forces of the actuators. Since the system is planar, the Lagrangian is the sum of the total kinetic energies of the two manipulator links, or:

$$\mathcal{L} = \mathrm{T}_1 + \mathrm{T}_2 = \frac{1}{2} m_1 \left(\dot{\bar{\mathrm{r}}}_1 \bullet \dot{\bar{\mathrm{r}}}_1\right) + \frac{1}{2} m_2 \left(\dot{\bar{\mathrm{r}}}_2 \bullet \dot{\bar{\mathrm{r}}}_2\right) + \frac{1}{2} \mathrm{I}_1 \dot{\theta}_1^2 + \frac{1}{2} \mathrm{I}_2 \left(\dot{\theta}_1 + \dot{\theta}_2\right)^2 + \frac{1}{2} n_2 l_1^2 \dot{\theta}_1^2 \tag{2}$$

where T_1 and T_2 are the kinetic energies of link 1 and link 2 and their associated motors, m_1 and m_2 are the masses of link 1 and link 2, $\dot{\bar{\mathrm{r}}}_1$ and $\dot{\bar{\mathrm{r}}}_2$ are the position vectors of the centers of mass of link 1 and link 2 relative to the inertial reference frame, I_1 and I_2 are the moments of inertia of link 1 and link 2, and n_2 is the mass of the actuator to be placed at joint 2. From Eq. (2), the expression for the Lagrangian can be obtained as:

$$\begin{aligned} \mathcal{L} = {} & \frac{1}{8} m_1 l_1^2 \dot{\theta}_1^2 + \frac{1}{2} \mathrm{I}_1 \dot{\theta}_1^2 + \frac{1}{2} m_2 l_1^2 \dot{\theta}_1^2 + \frac{1}{8} m_2 l_2^2 \left(\dot{\theta}_1 + \dot{\theta}_2\right)^2 \\ & + \frac{1}{2} m_2 l_1 l_2 \dot{\theta}_1 \left(\dot{\theta}_1 + \dot{\theta}_2\right) \cos\theta_2 + \frac{1}{2} \mathrm{I}_2 \left(\dot{\theta}_1 + \dot{\theta}_2\right)^2 + \frac{1}{2} n_2 l_1^2 \dot{\theta}_1^2 \end{aligned} \tag{3}$$

where l_1, l_2, θ_2, $\dot{\theta}_1$, and $\dot{\theta}_2$ are according to definitions in Fig. 2.

Substituting Eq. (3) into Eq. (1) the two dynamical equations are obtained as:

$$\tau_1 = \frac{d}{dt}\left(\frac{\partial \mathcal{L}}{\partial \dot{\theta}_1}\right) - \frac{\partial \mathcal{L}}{\partial \theta_1} \tag{4}$$

and

$$\tau_2 = \frac{d}{dt}\left(\frac{\partial \mathcal{L}}{\partial \dot{\theta}_2}\right) - \frac{\partial \mathcal{L}}{\partial \theta_2} \tag{5}$$

that can be simplified to yield:

$$\begin{aligned}\tau_1 = &\left[\frac{1}{4}m_1 l_1^2 + I_1 + m_2 l_1^2 + \frac{1}{4}m_2 l_2^2 + m_2 l_1 l_2 \cos\theta_2 + n_2 l_1^2 + I_2\right]\ddot{\theta}_1 \\ &+\left[\frac{1}{4}m_2 l_2^2 + \frac{1}{2}m_2 l_1 l_2 \cos\theta_2 + I_2\right]\ddot{\theta}_2 - \left[\frac{1}{2}m_2 l_1 l_2 \dot{\theta}_2\left(\dot{\theta}_1 + \dot{\theta}_2\right)\sin\theta_2 + \frac{1}{2}m_2 l_1 l_2 \dot{\theta}_1 \dot{\theta}_2 \sin\theta_2\right]\end{aligned} \tag{6}$$

and

$$\tau_2 = \left[\frac{1}{4}m_2 l_2^2 + \frac{1}{2}m_2 l_1 l_2 \cos\theta_2 + I_2\right]\ddot{\theta}_1 + \left[\frac{1}{4}m_2 l_2^2 + I_2\right]\ddot{\theta}_2 + \left[\frac{1}{2}m_2 l_1 l_2 \dot{\theta}_1^2 \sin\theta_2\right] \tag{7}$$

The goal of determining the above expressions for torque was to select the motor and reduction gear assemblies to be placed at the manipulator joints. Of primary interest was to calculate a value for the maximum required output torque of the actuators. Therefore, Eq. (6) and Eq. (7) were maximized term by term with the following results:

$$\begin{aligned}\tau_1 = &\left(\frac{1}{4}m_1 l_1^2 + I_1 + m_2 l_1^2 + \frac{1}{4}m_2 l_2^2 + m_2 l_1 l_2 + I_2 + n_2 l_1^2\right)\ddot{\theta}_1 \\ &+\left(\frac{1}{4}m_2 l_2^2 + \frac{1}{2}m_2 l_1 l_2 + I_2\right)\ddot{\theta}_2 + \left(\frac{1}{2}m_2 l_1 l_2\left(\dot{\theta}_1 + \dot{\theta}_2\right) + \frac{1}{2}m_2 l_1 l_2 \dot{\theta}_1\right)\dot{\theta}_2\end{aligned} \tag{8}$$

and

$$\tau_2 = \left(\frac{1}{4}m_2 l_2^2 + \frac{1}{2}m_2 l_1 l_2 + I_2\right)\ddot{\theta}_1 + \left(\frac{1}{4}m_2 l_2^2 + I_2\right)\ddot{\theta}_2 + \left(\frac{1}{2}m_2 l_1 l_2\right)\dot{\theta}_1^2 \tag{9}$$

The values for the dynamic parameters in Eq. (6) and Eq. (7) are found in Table 2. The values for l_1 and l_2 are found in Table 1. The upper bounds of the angular velocities and angular accelerations were chosen to encompass a wide range of feasible motion. Their values are listed in Table 2.

TABLE 2. VALUES OF THE DYNAMIC AND KINEMATIC PARAMETERS

	Link 1	Link 2
mass (kg)	1.614	1.009
I (kg·m^2)	0.660	0.331
$\lvert\dot{\theta}\rvert_{max}$ $\left(\text{rad}/\text{sec}\right)$	2.5	2.5
$\lvert\ddot{\theta}\rvert_{max}$ $\left(\text{rad}/\text{sec}^2\right)$	7.5	7.5

A factor of safety of 2.0 was incorporated to calculate the following values of maximum torque:

TABLE 3. REQUIRED MAXIMUM TORQUES AT THE MANIPULATOR JOINTS

	Newton-meters	ounce-inches
Torque 1	6.45	913
Torque 2	2.58	365

These values, along with the maximum values of angular velocity and angular acceleration presented in Table 2, were provided to an outside manufacturer for selection of the correct motor and reduction gear assemblies. The manufacturer selected an ideal reduction ratio to ensure the desired maximum values of torque, angular velocity, and angular acceleration were obtained at the output shaft of the gear box.

B. MECHANICAL COMPONENTS OF THE PLANAR SPACE ROBOT

In this portion of Chapter II., the individual components of the robot are examined in detail. Criteria for selection of each component is discussed. Also listed are the specifications [Ref. 9, Ref. 10, Ref. 11, Ref. 12], manufacturer, and costs.

1. The DC Brushless Motor/Harmonic Drive Gearbox/Optical Encoder Assembly and DC Brushless Servo Amplifier

DC Brushless motors have become common place in most robotics controls applications. DC brushless motors, due to the absence of brushes, enjoy a much longer operating life and can operate at higher speeds for longer periods of time. But one of the key properties of a DC brushless motor is that they produce large amounts of torque for a relatively small size as compared to a permanent magnet DC motor or a stepper motor. Once the torque requirements and reduction ratios were determined, an outside engineering firm was selected to manufacture a complete assembly consisting of the motor, harmonic drive, and optical encoder and to supply the DC brushless servo amplifier. Harmonic drive gearboxes are compact and produce a large reduction ratio from a single reduction pass. They have very low backlash and the type selected are rated as 97% efficient. Five hundred line incremental encoders were selected because they are optical and take advantage of the rotor position accuracy inherent to DC brushless motors. The amplifiers were designed specifically for operation with the MFM 032-.75 and 044-.5 used in this design. The model BDC 0250 series brushless servo amplifiers are four quadrant, 20 kHz PWM amplifiers that provide economical control of brushless motors rated from 1/3 to 2 Hp shaft Watts-out [Ref. 9].

The power for the motor amplifiers is provided by a 48 volt DC power supply that can deliver up to 12 amps of current. A stock power supply was purchased from an outside manufacturer. Electrical connections for the motors, encoders, and amplifiers will be discussed in Chapter IV.

Manufacturer information and specifications for the two motor actuator assemblies, the DC brushless amplifiers, and the amplifiers' power supplies are provided in the following two tables. [Ref 9, Ref. 10, Ref. 11]

TABLE 4. MOTOR ASSEMBLY AND AMPLIFIER SPECIFICATIONS

Component	Parameter	Assembly #1	Assembly #2
Motor	Designation	MFM-M044-.5	MFM-M032-.75
	Motor Constant	5.04 oz-in/$\sqrt{amps}$	3.12 oz-in/$\sqrt{amps}$
	Number of Poles	6	4
	Phase Connection	WYE	WYE
	Constant Output Torque	17.3 oz-in	9.2 oz-in
	Peak Output Torque	90.0 oz-in	40.2 oz-in
Gearbox	Designation	RH14-72-CC-SP	RH11-50-CC-SP
	Reduction Ratio	72/1	50/1
	Rated Output Speed	48.6 RPM	70 RPM
	Maximum Output Speed	69.4 RPM	100 RPM
	Rated Output Torque	1104 oz-in	352 oz-in
	Peak Repeat Output Torque	1856 oz-in	704 oz-in
Encoder	Designation	BEI-500 PPR	BEI-500 PPR
	Type	Optical	Optical
	Code	Incremental	Incremental
	Frequency Response	100 kHz	100 kHz
Motor/GB/Encoder	Weight	31 oz.	19 oz.
	Cost	$1875	$1537
Amplifier:	Designation	BDC 0251	BDC 0251
	Cost	$458	$458

TABLE 5. MOTOR ASSEMBLIES MANUFACTURER INFORMATION

DC Brushless Motor	MFM Technology, Inc. 200 Thirteenth Ave. Ronkonkoma, NY 11779 Ph: (516) 467-5151
Harmonic Drive Gearbox	HD Systems 89 Cabot Ct. Hauppauge, NY 11788 Ph: (516) 231-6630
Optical Encoder	BEI Motion Systems Co. 1755-B La Costa Meadows Dr. San Marcos, CA 92069 Ph: (619) 471-2600
Amplifier	MFM Technology, Inc. 200 Thirteenth Ave. Ronkonkoma, NY 11779 Ph: (516) 467-5151
Power Supply	Technology Dynamics Inc. 100 School St. Bergenfield, NJ 07621 Ph: (201) 385-0500

2. Bearings for Planar Motion

The space robot under consideration was modeled as a planar system. Therefore, to ensure proper operation of the system for the values calculated and assumptions used in developing the dynamical equations, the space vehicle and manipulator links must rotate in a plane parallel to one another. Needle thrust bearings

were selected due to their compact size. These bearings were purchased locally and added to the robot as depicted in Fig. 1(b) and Fig. 3. Since no thrust needed to be absorbed by the bearings, their sole purpose was to ensure that the vertical separation between the space vehicle and link 1 and between link 1 and link 2 was equal under all operating conditions. The following bearing information is provided. [Ref. 12]

TABLE 6. NEEDLE ROLLER BEARING SPECIFICATIONS AND INFORMATION

Distributor	Girardi Bearing Company 61 Chamberlain Street Salinas, CA 93901 Ph: (408) 422-5371	
Manufacturer	The Torrington Co. 59 Field St. Torrington, CT 06790 Ph: (203) 482-9511	
	Bearing #1	Bearing #2
Designation	NTA 2031	NTA 1423
Bearing Life	>40000 hrs	>40000 hrs
Static Load Rating	3690 lbf	2350 lbf
Dynamic Load Rating	18200 lbf	9200 lbf
Limiting Speed	8800 rpm	12000 rpm

III. SIMULATING A GRAVITY FREE ENVIRONMENT IN 2-D

In designing the facilities for this research, the difficult task of simulating a gravity free environment was accomplished by the use of an air cushion that minimized frictional effects. State of the art air pads are available in various shapes and sizes to accommodate complex and bulky systems as well as simple and relatively light weight systems such as the type designed as part of this thesis. In this chapter, the components which were selected, designed, and manufactured to obtain a free floating system, are examined.

A. SELECTION OF THE SPACE ROBOT AIR PADS

Air pads (or air bearings) are widely used throughout industry in numerous applications. The most common employment is in coordinate measuring systems which measure the dimensions of an object. In general, air bearings are utilized whenever precision motion is desired due to the fact that air bearings provide an essentially frictionless operating surface. Other common uses are laser plotting equipment, sophisticated testing equipment for use with semiconductors, as well as space systems applications.

The object of any air bearing system is to bring air under pressure between two surfaces in order to create a precise air gap. The characteristics of air bearings are functions of the geometry of the air distribution pattern and the air pressure. The air bearing has the great advantage of eliminating minor irregularities inherent in any ball or roller system, as well as virtually eliminating friction. Although magnetic bearings are gaining due recognition in creating the same effects, air pads enjoy the distinct advantages of simplicity and low cost.

A company, which specializes in air pads, was selected because of its state of the art systems. The main feature introduced by DEXTER PADS is the air flow control system that generates the air gap between the moving surfaces. The flow pattern offers stability

to the pads as well as provides a high load bearing capacity with low air consumption. Vibration is completely absent under normal working conditions. These properties are achieved by a combination of air diffusion through a porous ring, together with an interchangeable restrictor with a capillary orifice, located in the body of the pad as shown in Fig. 6. The restrictor is an auto-regulator. In its absence, a reduction of the load on the bearing would increase the thickness of the gap and consequently increase the air consumption. When the air flow increases the restrictor reduces the pressure in the air gap and controls the air gap thickness. Consequently, the restrictor increases the rigidity of the air bearing and has a damping effect. [Ref. 6]

The size of the orifice determines the varying bearing capacities, gap thickness, and air output. The total weight of the space robot and its accessories, which the system of air bearings would be required to support, was calculated to be 8 kg. A factor of safety of 1.5 increased the value to 12 kg, or roughly 26.5 lbs. The appropriate bearings were selected from information provided by the manufacturer. The pad is adjustable as well as articulated (Fig. 6). The adjustability was a desirable quality because it allowed the pad stems to be recessed into the body of the robot while still providing easy access for height adjustments. Articulation manifests itself in the form of a pivoting joint at the stem/air pad intersection that allows the pad to accommodate the unevenness of the surface on which it acts. This quality was ideal for its application in the design of the testbed since the operating surface selected was glass, which is inherently uneven.

It was imperative that the weight of the robot be evenly distributed among the bearings. Three bearings were decided upon because more pads would be redundant. The center of mass for the system was determined and the bearings were placed as illustrated in Fig. 1(a) and Fig. 1(b). Air is supplied to the bearings through inlet ports located on the sides of the air pads. A leveling device was manufactured to ensure equal heights were achieved among the three bearings. The robot was then placed on a flat surface. A telescoping micrometer was used to ensure less than .0001 mm error between bearing heights. The following information for the individual air pads is provided.

TABLE 7. AIR PAD INFORMATION AND SPECIFICATIONS

Distributor	AMEROPEAN Corporation 7 Corporate Drive, # 109 North Haven, CT 06473 Ph: (203) 239-0448
Manufacturer	DEXTER CONTINENTAL N.V. Industrial blok D1 B-9140 Zele - Belgium Ph: 052/44,57,54
Pad Designation	PD-RARA018
Pad Diameter	32mm
Nominal Load	12 kg
Supply Pressure	5 atmospheres
Air Gap	9-10 microns

Air was supplied to the bearings from house air. The air was passed through a 40 micron filter, then regulated to 5 atmospheres. The air was then passed through a cyclone water separator, desiccant dryer, and a 5 micron filter. Stock 1/8 inch ID plastic tubing was used to pass the air from the outlet of the filter to a series of plastic 'T' connections and into the air inlet port of the air pads.

B. GLASS TABLE AND SUPPORT STRUCTURE DESIGN

The air pads require a non-porous bearing surface with a maximum roughness of 0.2 μm or 8 microinches [Ref. 6]. The most common surface used in space robot controls is granite. But, granite tables are expensive and extremely heavy. In an attempt to minimize both, glass was selected as a suitable substitute. Glass is a non-porous surface and most grades of glass meet the roughness criteria. [Ref. 7] lists the quality

requirements for glass. One half inch thick glass is limited to a quality referred to as glazing select. One half inch thick glass can support point loads of 92 kg (~202 lbs) when the glass is supported at two foot increments. The glass, purchased from a local distributor cost, $428.

A support structure (basically a four legged table) for the glass was manufactured from aluminum angle. The upper structure has six lengths of angle running parallel to the plane of the glass. Four lengths make up the support for the edges of the glass, and two were placed at two foot increments and run the length of the glass as depicted in Fig. 4. This allowed supports to be placed at two foot increments underneath the glass in order to meet the point load requirements mentioned earlier. The supports are 5/16-24 allen head bolts. Teflon pads were manufactured to cover the rough end of the bolt to ensure no concentrated load was applied to the bolt's rough edges. The lower support structure has four legs perpendicular to the plane of the glass and four trusses at 45 degree angles for support of the upper structure which adds rigidity to the overall system. Each of the legs has an adjustable foot for gross leveling of the structure as seen in Fig. 4. The upper support structure has adjustable feet located at two foot increments for fine tune leveling also shown in Fig. 4. The entire assembly was manufactured at the Engineering and Machine Shop of the Naval Postgraduate School.

Leveling of the glass was accomplished in two steps. First, a gross level was performed using the adjustable feet at the bottom of the legs. A carpenter's level was placed at various locations and the feet were adjusted accordingly by visually placing the bubble at level. Second, air was applied to the robot. Visually imperceptible unevenness in the glass will cause a transverse drift in the robot. The two foot incremented leveling feet were adjusted to eliminate the robot's drift. As a measure of the impact the leveling feet have on the glass leveling adjustment, a quarter of a turn on the leveling feet will cause the robot to drift. The aluminum for the supporting table and the glass were purchased from a local distributor at a cost of $145.

IV. COMPUTER CONTROL OF THE SPACE ROBOT

The motivation behind this research began with the work presented in [Ref. 2]. Algorithms have been developed and more will be developed in the future which will require some type of experimental testbed for validation. This chapter describes the computer hardware and software of the experimental testbed. Figure 5 provides a block diagram of the components required as well as the path of information flow.

A. THE HOST COMPUTER, A SPARC STATION LX

The computer selected for this project was a SPARCstation LX. The SPARCstation is a UNIX based system which has a powerful and easy to use programming environment. The source program (or algorithm) is coded in C and written with the SPARCstation's editor. It is translated into an executable program by cross-compilation on the SPARCstation using the Texas Instrument C compiler and linker. The executable program is subsequently downloaded onto the Robot Controller Card (RCC) board via a downloader which uses RCC driver system calls [Ref. 13]. The RCC will be discussed in more detail in subsequent paragraphs but at this point of time it suffices to know that it is the real time computer that directly controls the robot. There are two translators that must be accessed to pass the information from the UNIX system to the RCC. One is the SBus Adapter and the second is the VME Adapter.

B. SBUS-TO-VME TRANSLATION

1. The SBus-to-VME Adapter

The ability of the SPARCstation to communicate directly with the RCC rests with the SBus-to-VME Adapter. The PT-SBS915 actually consists of an SBus Adapter Card and a VMEbus Adapter Card connected by a cable. The SBus Adapter is placed in

the workstation of the SPARCstation and the VMEbus Adapter is placed on the VMEbus. The two board set provides a master-slave interface between an SBus and a VMEbus backplane. The 915 allows an SBus master to access all VMEbus address spaces and act as a VMEbus Interrupt Handler. Conversely, a VMEbus master can access the SBus as a master. The PT-SBS915 maintains a high level of software transparency. [Ref. 14]

2. VME 512 Vertical Powered Rack

The VME 512 is a vertical load powered rack, designed to handle 12 VME backplanes. It has a 350 Watt power supply, cooling fan, and LED voltage indicator lights [Ref. 15]. The VME 512 powered rack serves as the common locator and power source for the VME slaved cards of the Robot Control System and provides the final translation path from the UNIX system to the RCC.

C. THE ROBOT CONTROL SYSTEM (RCS)

The heart of the required hardware and software is the Robot Control System (RCS), developed by a California engineering firm. The RCS is a homogeneous multiprocessor system that is designed to be powerful, flexible, and easy to use. The RCS meets these design goals in the following ways. Computational power can be added by simply plugging in additional CPU cards. Flexibility is achieved by having a modular system that can be easily partitioned among tasks at both the hardware and software levels. The RCS is accessed through the UNIX system, providing a powerful and easy to use programming environment. [Ref. 13]

1. The Robot Controller Card (RCC)

Recalling that the robot is controlled in real time, the center piece of the RCS is the Robot Controller Card (RCC). The RCC is a TI320C31 DSP based, real time computer that operates up to 33 MHz, has 4 Mb of RAM, and provides up to 33MFLOPS of performance. User programs are developed on the host system and downloaded to the RCC via device drivers. The executable program usually runs on the RCC without help from the host, except when remote IO is needed on the host (such as scanf and printf). In

the latter case, the RCC communicates and synchronizes with the host which carries out the IO operation on the RCC's behalf. The RCC can also interrupt the host over the VME bus at any of seven interrupt levels. [Ref. 13]

2. The RCC-VME Interface

VME are the initials for the bus structured backplanes that came out of the Versa-Module-Europa consortium [Ref. 15]. The VME is a bus that acts as the path and translator of information between the host system and the RCC. Thus, the RCC is a VME slave and interrupt generator. The VME is a standard configuration which developers of hardware and software may utilize to communicate with existing systems.

3. The Analog/Digital Card

The DC brushless motors used in the testbed are analog. The RCC provides digital output. Therefore, a digital to analog conversion must take place. The Analog/Digital Card (ADC) provides a flexible easy to use input/output capability. The ADC has nine DAC's for analog output that can be configured for either +/- 5V or +/- 10V operation. The DC brushless motors and servo amplifiers of the testbed require +/- 10V. The ADC has a single analog to digital converter, with eight channels, that may be used in circumstances when a digital feedback system is not employed. [Ref. 13]

4. The Position/Velocity Card

The Position/Velocity Card (PVC) provides position and velocity feedback from the optical encoder inputs. The PVC has six channels to convert quadrature encoder input to a 24bit position count. Velocity is also derived from the quadrature input signals by measuring time between the rising edges of one input signal. The result is the inverse of velocity. [Ref. 13]

5. The Input/Output Bus

Input and output for the RCS is handled through dedicated cards which are available to the RCC or host system. Communication with these input/output cards is done over a custom backplane that contains a privately defined bus system called the

IOBus (IOB). The IOB is the private bus system of the RCS. Cards can be easily designed to meet the IOB protocol and thus work with the RCS system. The ADC and PVC are two examples. [Ref. 13]

6. Software Library

The Robot Control System software was designed to allow the programmer to develop code for the RCC in order to enhance the available applications. The software is located in the SPARCstation's directories. Although a complete listing of the library functions, macros, and utility programs are maintained in the RCS operating manual [Ref. 13], some of the major directories are listed below.

- /usr/local/bin - The RCC executable directory. This directory contains the host executable files that aid in developing RCC software. To describe a few:

  runrcc - allows downloading and execution of an RCC executable program;

  monrcc - is a monitor program that runs on the SPARCstation. It allows access to the different RCC board resources (registers, memory, etc.) from the SPARCstation. From it, RCC memory patching, testing, and dumping can be performed. It also allows starting and stopping the processor;

  dumpit - is a utility program that "dumps" or displays an RCC executable program in readable form.

- /home/terminator/rcc/IO - Contains the following subdirectories:

  ADC - contains programs for testing the ADC;

  PVC - contains programs for testing the ADC;

  SERVOb - contains programs that do PID servoing on a motor wired to the ADC and PVC cards. The programs can be used as the basis for more complicated applications.

- /home/terminator/rcc/PROGb/C - This directory contains C programs for testing the RCC resources. Programs to turn on the LEDs, access the IO bus that has the ADC and PVC, activate interrupts, and use the remote IO on the SPARCstation (e.g., printf and scanf).

Numerous macros exist for the RCC, ADC, and PVC that provide the user with simple commands for changing channels (selects motor to be controlled), clearing channels, reading encoder velocities, printing, scanning, and timing. The library functions, macros, and utility programs are extensive. The RCS operating manual [Ref. 13] contains detailed descriptions of all available commands.

D. INFORMATION FLOW PATH

In an attempt to bring all of the above components together, the final flow path of information follows. An algorithm, or source program, is written at the SPARCstation where it is compiled and transferred to the RCC via the SBus-to-VME Adapter. The RCC is a real time computer that executes the compiled algorithm. The RCC generates the necessary digital commands for the actuators. These commands are converted into analog signals by the DAC in the Analog/Digital Card. The signals are amplified by the servo amplifier before being passed to the motors. Optical encoders detect the actual motor displacement and pass the information back to the RCC via the PVC. Along with position the PVC also computes the motor velocity for error determination. The RCC may then compute an error signal and update the motor positions as required.

E. COMPONENT MANUFACTURERS AND INFORMATION

The following table lists manufacturers' addresses, designations, and costs of the major components of the hardware and software described in this chapter.

TABLE 8. COMPUTER CONTROL MANUFACTURERS AND INFORMATION

SPARCstation	Manufacturer	Sun Microsystems, Inc. 2550 Garcia Ave. Mountain View, CA 94043 (415) 960-1300
	Designation	SPARCstation LX
	Cost	$6,000
SBus-to-VME Adapter	Manufacturer	Performance Technology, Inc. 315 Science Pkwy Rochester, NY 14620 (716) 256-0200
	Designation	PT-SBS915
	Cost	$2,395
VME 512 Vertical Powered Rack	Manufacturer	MUPAC Corporation 10 MUPAC Dr. Brockton, MA 02401 (508) 588-6110
	Designation	5127FCF12AC-003
	Cost	$2,200
Robot Control System	Manufacturer	Computer Motion, Inc. 250 Stroke Rd., Suite A Goleta, CA 93117 (805) 685-3729
	Designation	Robot Control System
	Cost	$20,000

V. SUMMARY AND RECOMMENDATIONS

A. SUMMARY

In this thesis, an experimental testbed for testing existing algorithms and algorithms to be developed in the future was designed, constructed, and tested. As with all experimental apparatus, the final product was in some ways changed from the initial design. The initial design was built with five air pads. After considerable effort to balance the space robot, one air pad was removed and eventually a second pad was removed. The robot's motion was easier to control but the nominal load capacity of the system of air bearings had been exceeded. Further iterations led to replacing the 24mm air pads with 32mm pads, capable of supporting twice the load per bearing. The air pads purchased also began to show signs of rust and deposits on the pad surface as well as along its sides. Although the recommended particulate filters and water separator had been employed, a desiccant dryer was added to the air supply system to ensure minimal vapor accumulation in the air being passed to the pads. The second of the iterations led to a combined mass of 6500 grams (roughly 12 lbs) of aluminum being machined from the space vehicle and the two links. Past research recommends the sum of the masses of the links and associated actuators be less than 30 percent of the total mass of the system. After the robot's weight had been reduced, the ratio was calculated to be 32 percent. Removing more mass would have affected the locations of some of the threaded holes required by several components..

The needle roller bearings were added to the facility after parallel motion of the links and space vehicle relative to the glass operating surface became unattainable. With this particular iteration came a new and final method for mounting the motors to the links and space vehicle which added rigidity to the space robot as well as ease of disassembly.

Finally, a test program was executed which ensured the correct signals were being passed to the motors that ensured the encoders were returning the feedback signals necessary to update the robot's position. The space robot works as designed and is ready for testing the algorithm developed in [Ref. 2], future algorithms to be developed, and is ready for further research and experiments.

B. RECOMMENDATIONS

The use of the testbed for testing algorithms was the primary motivation for its construction. But, the testbed was also designed with expandability in mind. The first expansion should be to add a feedback system which ascertains the space robots position and orientation relative to an inertial reference frame. The algorithm developed in [Ref. 2] is an open loop control for motion planning and does not require feedback information. Feedback can be introduced through the addition of a gyroscope or flux gate compass or combination of the two, or through some type of vision system. Vision systems, currently in use through industry, are optical and infrared. Sonar, as a positioning device, is also an option. This facility can also be utilized to test algorithms currently under development for nonholonomic systems in general. In summary, the facility developed as part of this thesis has immediate as well as future uses and offers a wide range of possibilities for its deployment.

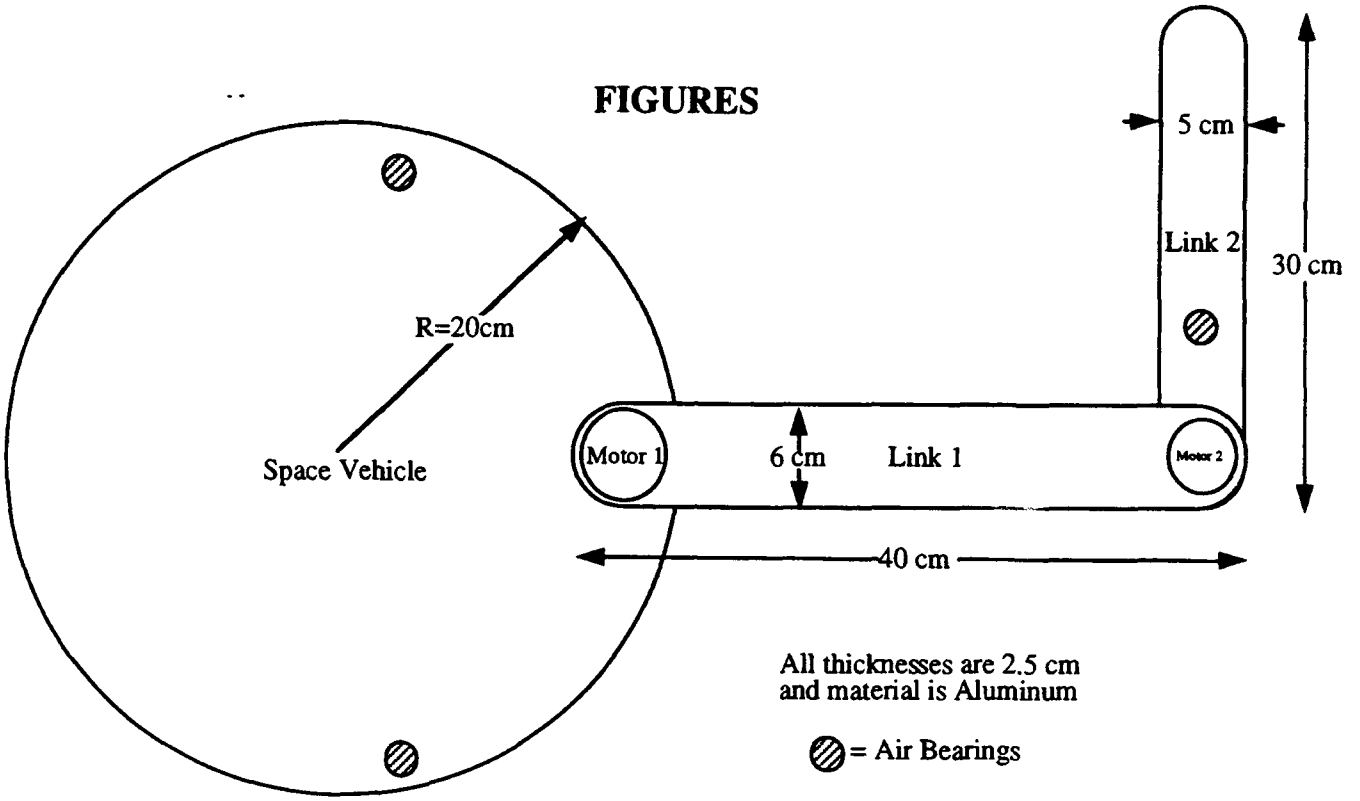

Figure 1(a). The Top View of the Space Robot.

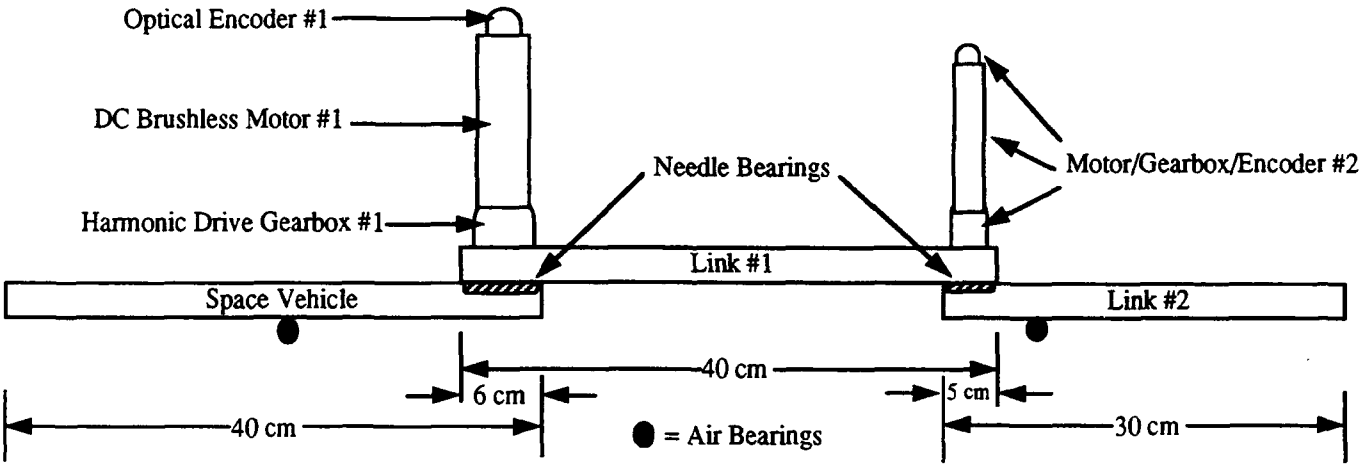

Figure 1(b). A Side View of the Space Robot.

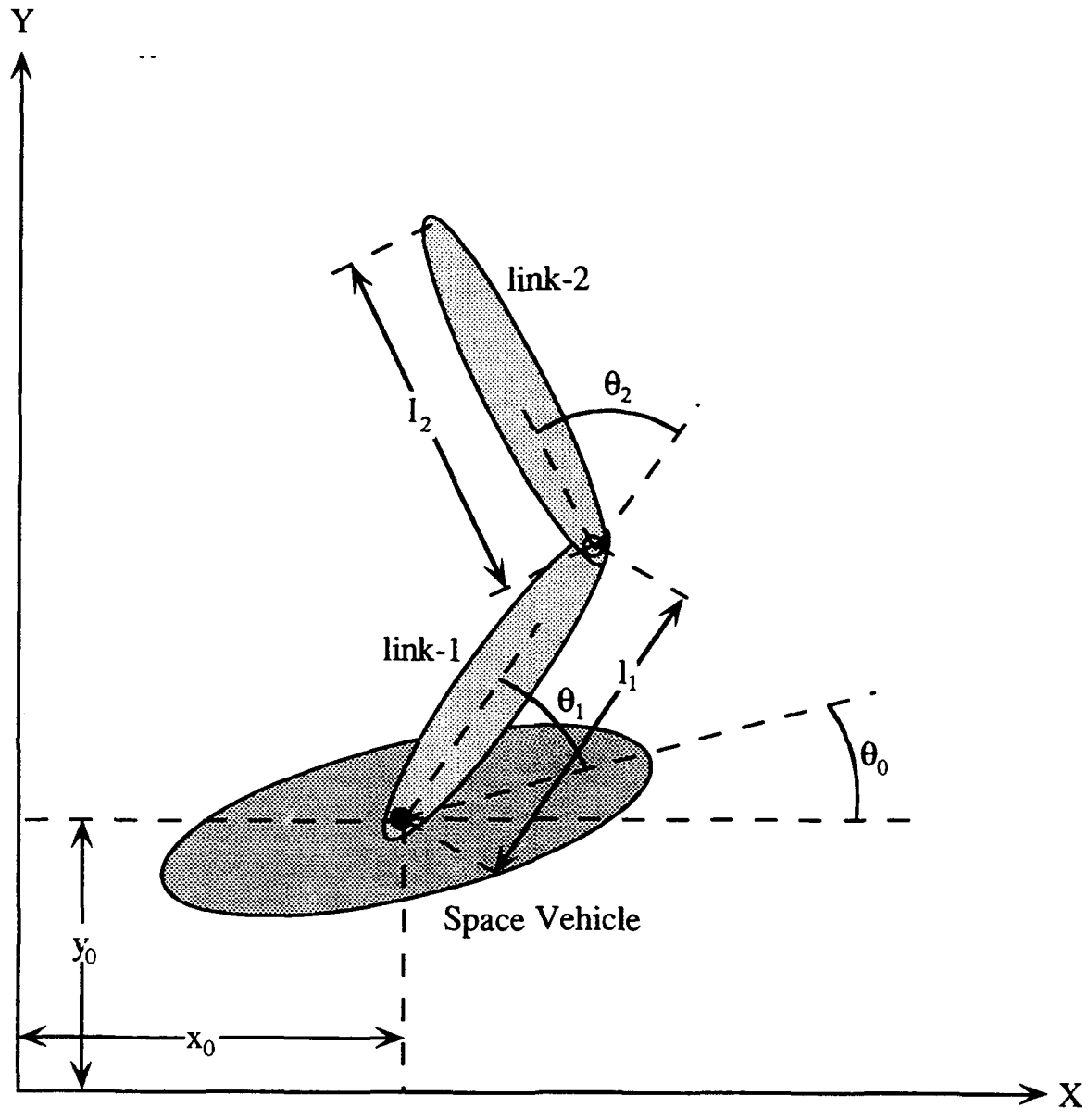

Figure 2. A Two-Link Manipulator Mounted on a Space Vehicle is Described by Three Generalized Coordinates: θ_0, θ_1, and θ_2. The Center of Mass of the Space Vehicle has the Coordinates x_0 and y_0.

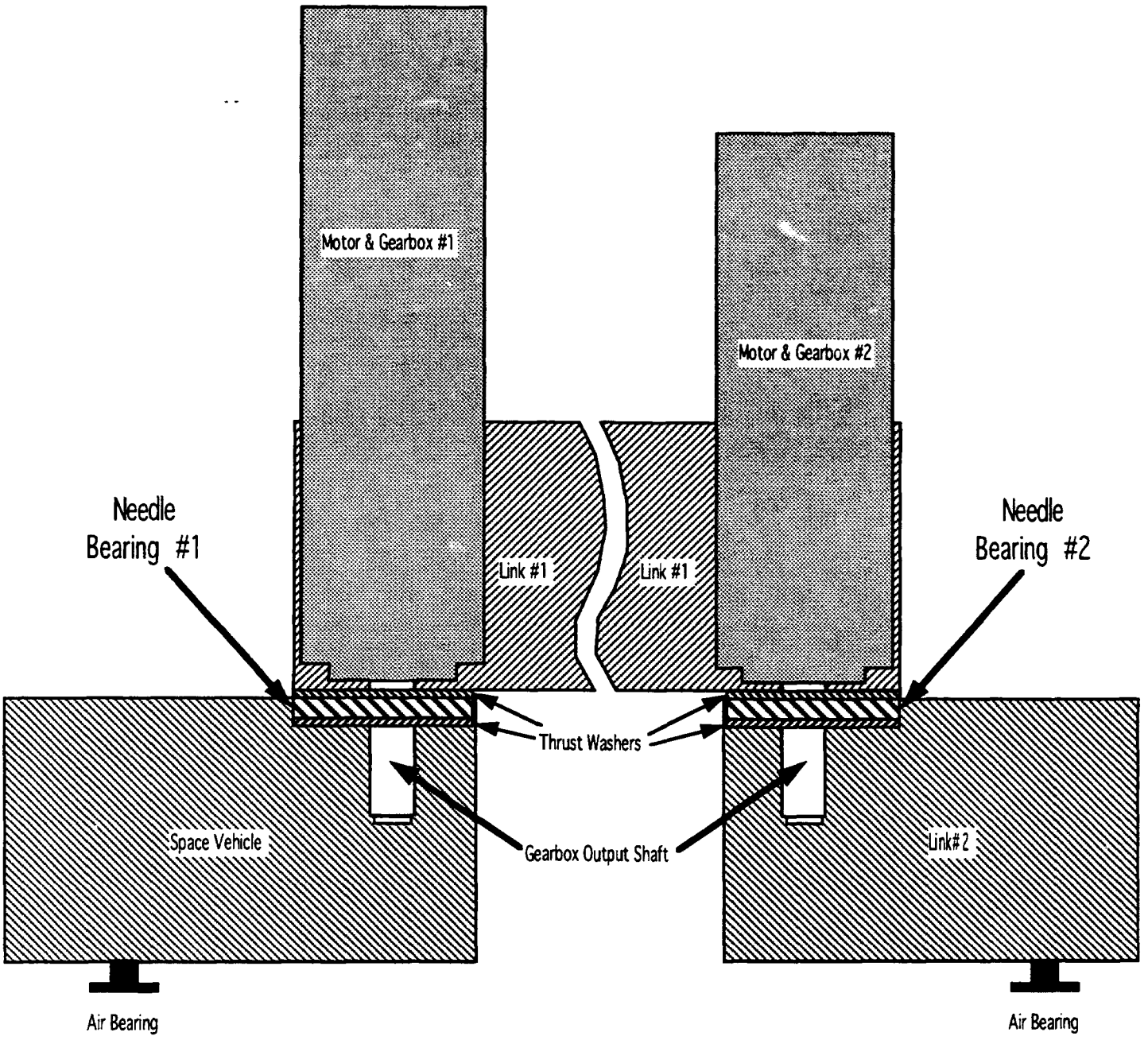

Figure 3. Needle Roller Bearings #1 and #2.

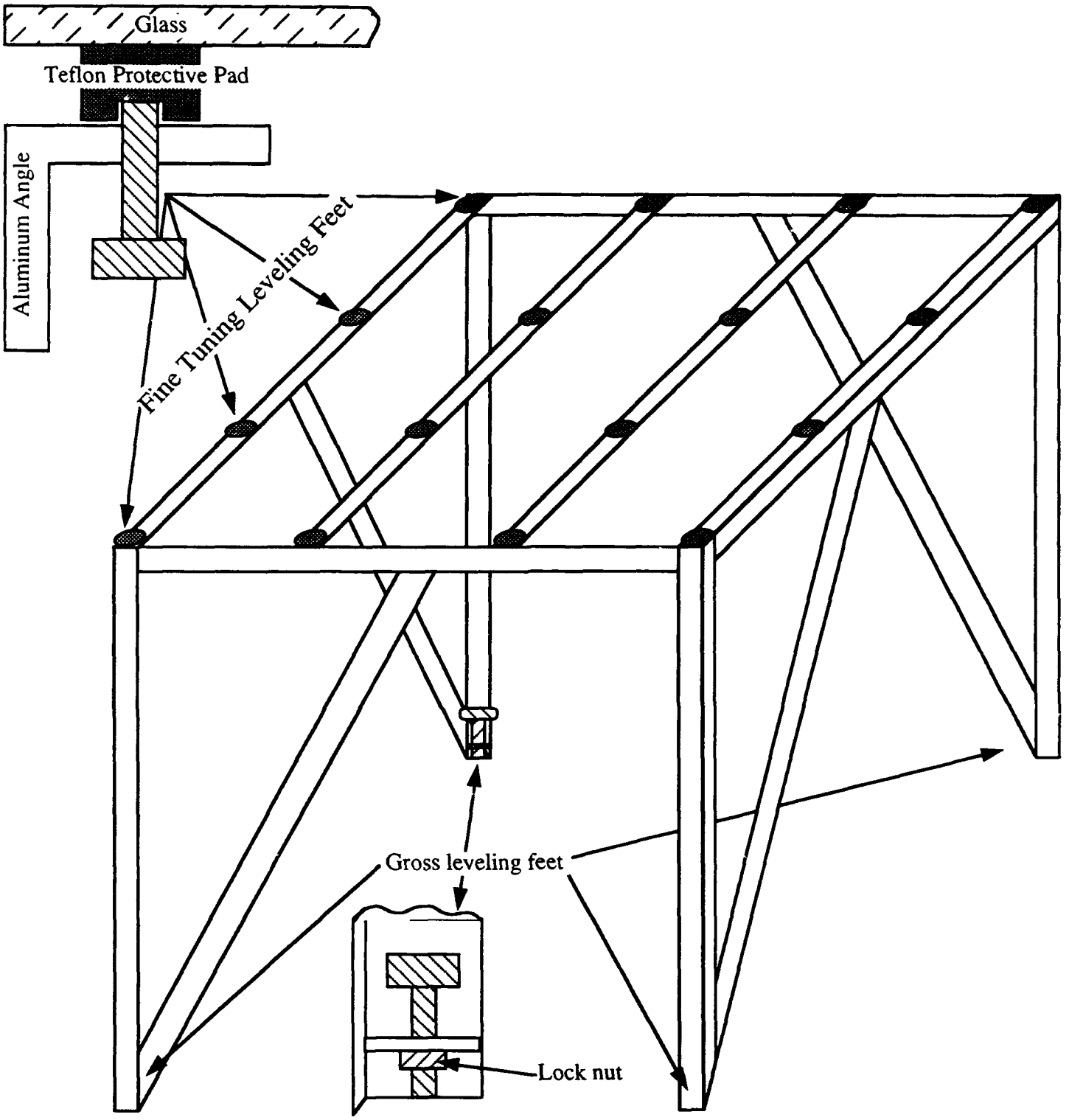

Figure 4. Glass Table Support Structure with Close-Up of the Fine Tuning Leveling Feet and the Gross Leveling Feet.

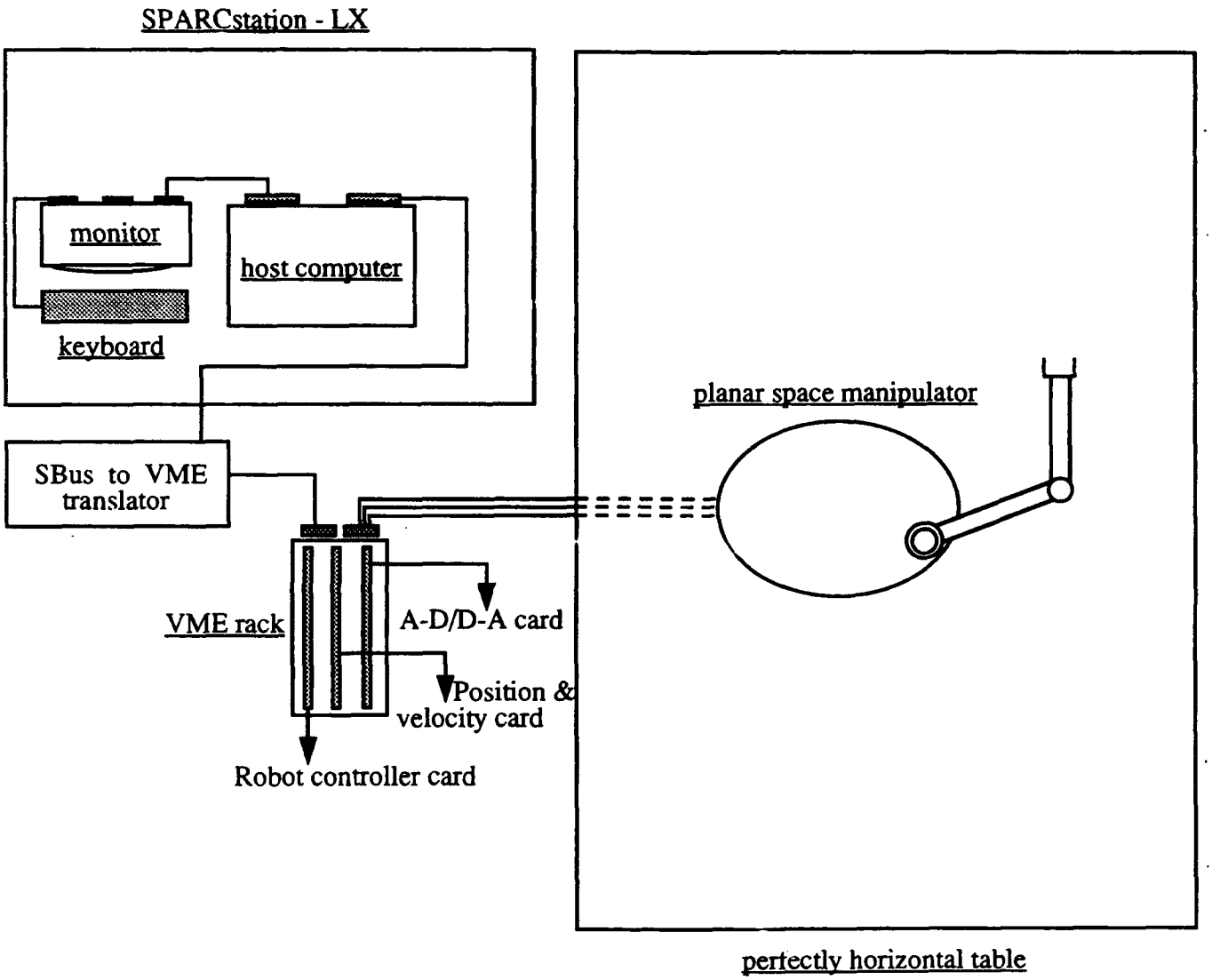

Figure 5. Computer Control System Block Diagram

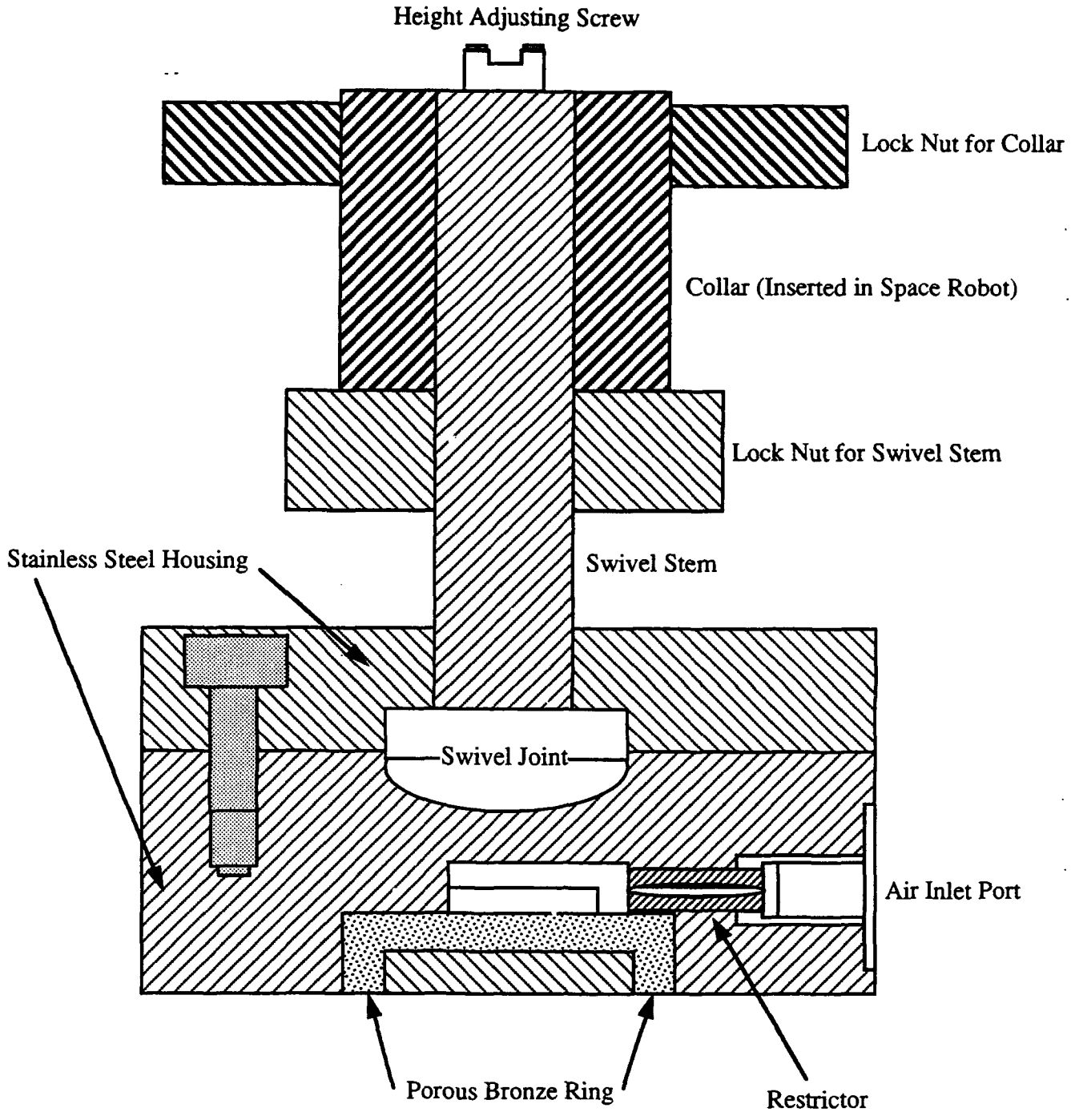

Figure 6. DEXTER PDRARA Articulated-Adjustable Air Pad

REFERENCES

1. Fernandes, C., Gurvits, L., and Li, X.Z., *Foundations of Nonholonomic Motion Planning*, paper presented at the IEEE International Conference on Robotics and Automation: Workshop on Nonholonomic Motion Planning, Sacramento, CA, April 1991.

2. Anderson, D.P., *A Surface Integral Algorithm for the Motion Planning of Nonholonomic Systems*, Master Thesis, Naval Postgraduate School, Monterey, CA, December 1992.

3. Nakamura, Y., and Mukherjee, R., *Nonholonomic Path Planning of Space Robots via a Bidirectional Approach*, IEEE Transactions on Robotics and Automation, v.7, no. 4, pp. 500-514, August 1991.

4. Vafa, Z., and Dubowsky, S., *On the Dynamics of Manipulators in Space Using the Virtual Manipulator Approach*, IEEE International Conference on Robotics and Automation, v.1, pp. 579-585, 1987.

5. Asada, H., and Youcef-Toumi, K., *Direct-Drive Robots Theory and Practice*, The MIT Press, 1987.

6. AMEROPEAN Corp., Specification PDRARA 032mm, *DEXTER ™ Pads for Bearings*, AMEROPEAN Corp., New Haven, CT, 1993.

7. American Society for Testing and Materials, Specification C 1036-90, *Standard Specification for Flat Glass*, April 1990.

8. Greenwood, D.T., *Principles of Dynamics*, 2d ed., Prentice-Hall, Inc., 1988.

9. MFM Technology, Inc., Specification BDC 0251, *BDC 0251 DC Brushless Servo Amplifier*, MFM Technology, Inc., Ronkonkoma, NY, 1993.

10. MFM Technology, Inc., Specification M & K Series Brushless DC Motors, *Brushless DC Motors*, MFM Technology, Inc., Ronkonkoma, NY, 1993

11. BEI Motion Systems Co., Specifications MOD5500/5600 Series, *MOD5500/5600 Enclosed Optical Encoder Module*, BEI Motion Systems Co., San Marcos, CA, 1992.

12. The Torrington Co., Specifications for Bearings, *Service Catalog*, 1st ed., 4th printing, The Torrington, Co., Torrington, CT, 1988.

13. Computer Motion Inc., Specification RCS, *The Robot Control System*, Computer Motion Inc., Goleta, CA, 1993.

14. Performance Technology, Inc., Specification Document Number 106A0183, *User's Manual PT SBS915 SBus-to-VMEbus Adapter*, Performance Technologies, Inc., Rochester, NY, 1993.

15. MUPAC Corp., Product Catalog, *Systems Packaging Products*, MUPAC Corp., Brockton, MA, 1992.

INITIAL DISTRIBUTION LIST

1.	Defense Technical Information Center Cameron Station Alexandria, VA 22304-6145	2
2.	Library, Code 52 Naval Postgraduate School Monterey, CA 93943-5002	2
3.	Department Chairman, Code ME Department of Mechanical Engineering Naval Postgraduate School Monterey, CA 93943-5000	2
4.	Professor R. Mukherjee, Code ME/Mk Department of Mechanical Engineering Naval Postgraduate School Monterey, CA 93943-5000	3
5.	Curricular Officer, Code 34 Department of Naval Engineering Naval Postgraduate School Monterey, CA 93943-5000	1
6.	LT Douglas L. Maddox Puget Sound Naval Shipyard 1400 Farragut Ave. Bremerton, WA 98314-5001	5